
BACKGROUND MATTING

A PREPRINT

Hossein Javidnia

ADAPT Centre

School of Computer Science and Statistics
Trinity College Dublin, Ireland
javidnih@tcd.ie

François Pitié

Sigmedia Group

Department of Electronic & Electrical Engineering
Trinity College Dublin, Ireland
pitief@tcd.ie

February 12, 2020

ABSTRACT

The current state of the art alpha matting methods mainly rely on the trimap as the secondary and only guidance to estimate alpha. This paper investigates the effects of utilising the background information as well as trimap in the process of alpha calculation. To achieve this goal, a state of the art method, AlphaGan is adopted and modified to process the background information as an extra input channel. Extensive experiments are performed to analyse the effect of the background information in image and video matting such as training with mildly and heavily distorted backgrounds. Based on the quantitative evaluations performed on Adobe Composition-1k dataset, the proposed pipeline significantly outperforms the state of the art methods using AlphaMatting benchmark metrics.

Keywords GAN · Alpha Matting · Foreground Extraction

1 Introduction

Alpha estimation is a regression problem that calculates the opacity value of each blended pixel in the foreground object. It serves as a prerequisite for a broad range of applications such as movie post production, digital image editing and compositing live action.

Formally, the composition image I_i is represented as a linear combination of the background B_i and foreground F_i colors [1]:

$$I_i = \alpha_i F_i + (1 - \alpha_i) B_i \quad (1)$$

where $\alpha_i \in [0, 1]$ denotes the opacity or alpha matte of the foreground at pixel i . Often, a user input is provided as a guidance in the form of a trimap, which assigns a label for every pixel as foreground $\alpha = 1$, background $\alpha = 0$ and unknown opacity. The goal of the matting algorithms is to estimate the unknown opacities by utilising the pixel color information of the known regions. Tackling the inverse problem of Eq. 1 is considerably difficult as there are 7 unknowns and 3 equations to be solved for an RGB image. The main motivation in this paper is to increase the matting accuracy by reducing the number of unknowns in Eq. 1. To do so, we presume that the background information B , is known either by capturing a clear background or through reconstruction methods that can estimate the occluded background regions.

In traditional methods, the matte is estimated by inferring the alpha information in the unknown areas from those in known areas [2]. For example, the matte values could be propagated from known to unknown areas based on the spatial and appearance affinity relation between them [3, 4, 5, 6, 7, 8, 9, 10]. An alternative solution is to compute the unknown mattes by sub-sampling the color and texture distribution of the foreground and background planes followed by an optimization such as likelihood of alpha values [1, 11, 12, 13, 14]. Despite the promising performance of these methods on public benchmarks, there is still an unresolved issue of natural image matting and consistency in videos between consecutive frames. One important reason causing this problem is the fact that the performance of these methods heavily rely on the accuracy of the given trimap. Generating the trimap for a sequence of images from a video is indeed a challenging task as it requires tracking the object of interest and defining an appropriate and relevant unknown areas to be solved.

To address these challenges, this paper presents a Background-Aware Generative Adversarial Network (AlphaGan-BG) which utilises the information present in the background plane to accurately estimate the alpha matte compensating for the issues caused by inaccurate trimap. Unlike the state of the art which only use RGB image and trimap as the input, AlphaGan-BG analyses the color and texture provided as background information to achieve a better accuracy. To our best knowledge, this paper contributes the first deep learning approach which takes advantage of the background information to estimate alpha mattes. Both our qualitative and quantitative experiments demonstrate that AlphaGan-BG significantly outperforms the state of the art matting methods.

2 Previous Works

Alpha matting is a well established and studied field of research in computer vision with a rich literature. A significant amount of work has been done over the past decade to address the issues in natural image matting. More recently, deep learning approaches have shown an impressive performance on various computer vision tasks including image matting too.

This section briefly reviews the state of the art alpha matting methods within two categories: conventional methods and deep learning based methods.

2.1 Conventional Matting Methods

The conventional alpha matting approaches could be categorised into sampling based and affinity based methods. Sampling based methods [1, 15, 12, 16] initially collect a set of known foreground and background color samples to identify the best foreground-background color pair for a pixel.

The general rule is to use Eq. 1 to calculate the alpha value once the corresponding background and foreground colors are determined. The issue with the sampling based method is that they don't make use of the texture information present in the image and they don't enforce spatial smoothness thus introducing an additional spatial smoothness step. More importantly, there is always the ambiguity on how the samples are chosen and where are they chosen from; causing matte discontinuities. For instance, Shared Matting [15] select the samples from the trimap boundaries between the known and unknown pixels. Global Matting [12] makes use of all the pixels within the trimap boundary therefore increasing the performance time. Sparse sampling [17] applies the sampling in a super-pixel level by assessing their similarity using KL-Divergence based distance measure.

Affinity-based methods work by analysing the affinities of neighboring pixels to propagate alpha information from known to unknown regions. Levin et al. [8] proposed a closed-form matting solution where the local color information is used to compute the affinity between two pixels. In [8] the alpha matte is calculated by solving a sparse linear system. The advantage of the closed-form solution is the prediction of the properties of the solution by analysing the eigenvectors of a sparse matrix. Chen et al. [18] proposed a locally linear embedding system which represents every unknown pixel as a linear combination of its neighbors. KNN matting [4] utilised nonlocal principal to find the affinities. The basis of this principal is that a pixel is a weighted sum of the pixels with similar appearance to the given weight [4]. This method enforces the the pixels and their corresponding nonlocal neighbors to have close alpha value. Aksoy et al. [3] constructed their method based on color-mixture flow using pixel-to-pixel connections between the image and it's corresponding trimap. The flow is based on local linear embedding with gradual improvement in matting quality as more building blocks are added to the information flow. It was shown in [3] that combining local and non-local affinities can result in a higher quality alpha matte. Several other state of the art approaches such as Random Walks [19], FuzzyMatte [20], Spectral Matting [9] and Geodesic Matting [21] can also be categorised as affinity based methods.

2.2 Deep Learning Based Matting Methods

Emerging field of deep learning along with the new generation of hardware, enabled many researches to tackle the issues of natural image matting with promising performances. Cho et al. [22] proposed an end-to-end Deep Convolutional Neural Networks (CNN) which utilises the results of the closed form matting and KNN matting for alpha estimation. Xu et al. [23] proposed a two part structure to predict alpha. The first part is an encoder-decoder module trained to predict the alpha from the input image and trimap; the second part is a small CNN trained to perform a post-processing step to increase the quality of the estimated alpha. Lu et al. [24] proposed IndexNet Matting by introducing indexed pooling and upsampling operators. They modeled the indices as a function of the feature map to perform the upsampling. There are many other methods proposed to use deep learning to tackle the issues of natural image matting such as VDRN Matting [25], SampleNet Matting [26], AdaMatting [27], Late Fusion Matting [28], Inductive Guided Filter Matting [29], however, the analysis of these methods goes beyond the scope of our work.

3 AlphaGan-BG Network

The framework in this research is built on the first proposed GAN to estimate alpha mattes. AlphaGAN [30] was introduced in 2018 motivated by the encoder-decoder structure proposed in [23]. The original architecture of AlphaGAN consists of a generator G and discriminator D .

In the original form of AlphaGAN, G accepts the input in a form of a 4 channel volume made of a composited image (3 channels) and the corresponding trimap (1 channel). D is responsible for distinguishing the real from fake input volume. The first 3 channels of the input volume to D belongs to the RGB values of the new composited images based on predicted alpha and the last channel is the original trimap to help D focus on salient regions.

AlphaGAN followed the same path as the rest of the state of the art methods with the assumption that the only data available is an RGB image and the corresponding trimap. However, in this paper, background information is also considered as the known variable and the input to the network.

3.1 Generator G

In this research, G is an encoder-decoder network that accepts the input in a form of a 7 channel volume, where the first 3 channels contain the RGB image, the second 3 channels contain the RGB background information and the last channel contains the trimap. The encoder is based on ResNet50 [31] architecture pretrained on ImageNet [32] where the convolutions in the 3rd and 4th block of the ResNet are replaced by dilated convolutions with rate 2 and 4, respectively. To resample features at several scales, Atrous Spatial Pyramid Pooling (ASPP) module [33, 34] is added after ResNet block 4.

Similar to AlphaGAN, the decoder is simply a set of convolutional layers and skip connections from the encoder. The output of the encoder is bilinearly upsampled with the factor of 2 to maintain the same spatial resolution for the feature maps as the output of ResNet block 1. To reduce the dimensions, the output of the ResNet block 1 is fed into 1×1 convolutional layer and concatenated with the upsampled feature maps from encoder. This is followed by 3×3 convolutions and upsampling using the saved pooling indices in the first layer of the encoder. The results are once again concatenated with the feature maps from the encoder with the same resolution. Before feeding the output to the final set of convolution layers, transposed convolutions are applied to upsample it followed by a concatenation with the RGB input image. ReLU [35] activation functions and Batch Normalization [36] layers are used for all the layers except the last one which utilises a sigmoid activation to scale the output between 0 and 1. Fig. 1 illustrates the encoder-decoder structure of G .

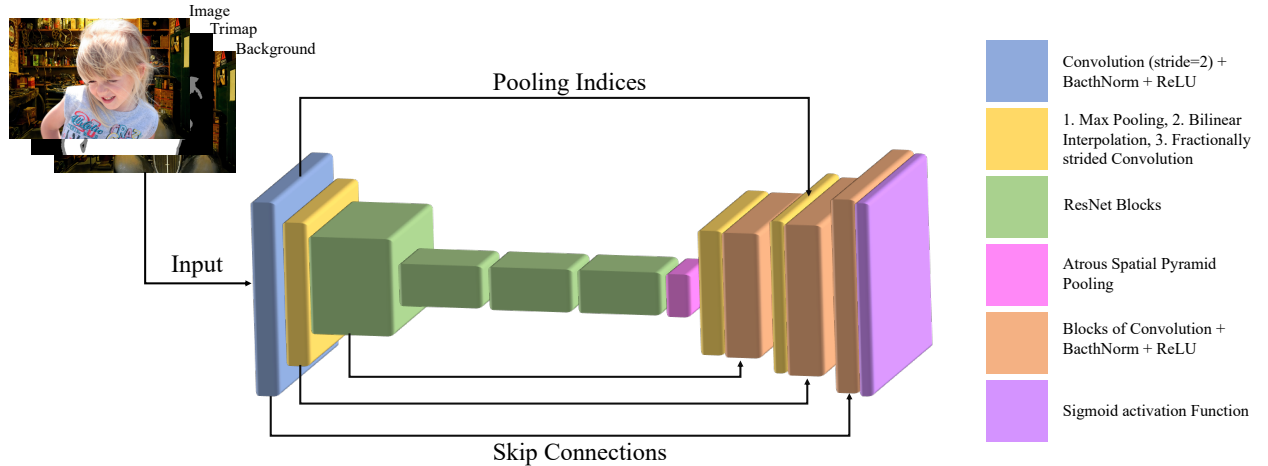


Figure 1: AlphaGan-BG: Structure of Generator (G).

3.2 Discriminator D

This architecture employs PatchGAN [37] as the discriminator. D attempts to distinguish fake from real input which is a 7 channel volume. The real input is constructed by original composition using truth alpha, background and trimap. The fake input contains the new composition using the alpha generated by G , background and the trimap. By providing the background information, D will enforce G to output sharper and more accurate result as the issue of differentiating foreground and background is resolved by default.

3.3 Loss Functions

The full objective of the network is a combination of three loss functions: alpha-prediction loss \mathcal{L}_{alpha} , compositional loss \mathcal{L}_{comp} and adversarial loss \mathcal{L}_{GAN} [38]:

$$\mathcal{L}_{total} = \mathcal{L}_{alpha} + \mathcal{L}_{comp} + \mathcal{L}_{GAN} \quad (2)$$

\mathcal{L}_{alpha} is the absolute difference of the ground truth and predicted alpha values for all the pixels. \mathcal{L}_{comp} is the absolute difference of the composited image using ground truth alpha and the composited image using predicted alpha. The composition in both cases are based on the ground truth foreground and background images [23]. \mathcal{L}_{GAN} is defined based on the fundamentals of adversarial networks, where in this research, G aims at generating alpha mattes close to the ground truth while D aims at distinguishing real from fake input; resulting in G minimizing the \mathcal{L}_{GAN} .

4 Experiments and Discussion

4.1 Dataset

The network in this paper is trained on Adobe Matting dataset [23] consists of 431 foreground images for training and 50 images for testing with corresponding ground truth. To augment the data, Pascal VOC 2008 [39] and MSCOCO images [40] are used as the background for image composition resulting in a training set containing 43100 images.

4.2 Data Preparation

As described in Section 3, this network takes advantage of the background information to predict alpha matte. This requires the background information to be available during the test phase as well as training. However, acquiring the background image during the test phase is a challenging task. To achieve this, several inpainting and background reconstruction methods [41, 42, 43, 44, 45, 46] are studied to analyse their accuracy and performance on static images and videos. The findings indicate that currently there is no background reconstruction method that can generate a clear background without artifacts. The ultimate goal is to obtain a reconstructed image which is equivalent of the original input used for the composition. The common artifacts present in the output of the reconstruction methods are the blur (degraded quality) and shift (translation), meaning that the region containing the object of interest is slightly translated in the reconstructed image.

To simulate these artifacts, two sets of backgrounds are augmented. In the first set, a random selection of images are manipulated by applying a hexagonal shape Gaussian blur with a random filter size. The location of the hexagonal blur is randomly chosen along the dimensions of the input image. The diameter of the shape is randomly selected between 120 and 345 pixels with rotation angle chosen by generating a linearly spaced vector. The blurred region is also translated using a 2D linear translation. In the second set, all the images are initially blurred followed by applying the hexagonal shape Gaussian blur at a random location. Comparatively, the first scenario represents a more realistic case as it contains both clean and partially distorted backgrounds. However, the second set represents severely distorted cases where all the images are blurred with an additional distorted patch introducing a more challenging set for training.

4.3 Training

In this paper, two models are trained for evaluation purposes. The first model utilises the first set of background images as described in Section 4.2 and the second model uses the second set of backgrounds with severe distortion. In order to make the remaining sections easier to follow, we refer to the first model as *AlphaGan-BG_M* (Mildly distorted) and second model as *AlphaGan-BG_H* (Heavily distorted).

AlphaGan-BG_M and AlphaGan-BG_H are trained for 376 and 650 epochs respectively with the initial learning rate set to 0.0002. Adam optimizer [47] with $\beta = 0.999$ is also employed for optimization purposes.

4.4 Results and Evaluation

4.5 Still Image Matting

The evaluation for still images is performed on a set of 50 images from Adobe Matting [23] test set. Note that, none of the test images are considered as part of the training. Four metrics based on AlphaMatting benchmark [48, 49] are used for evaluation purposes including Sum of Absolute Difference (SAD), Mean Square Error (MSE), Connectivity (CONN) and Gradient Errors (GRAD). The test images from AlphaMatting benchmark are not considered as part of this evaluation as there is no available background information for the test set. The background images used for

evaluation are also manipulated using the pipeline describes in Section 4.2 to simulate the reconstruction artifacts. The performance of the trained models are compared against 8 state of the art methods ranked in AlphaMatting benchmark with publicly available code including Closed-Form Matting [8], DCNN Matting [22], Deep Matting [23], IndexNet Matting [24], Information-flow Matting [3], KNN Matting [4], Late Fusion [28] and AlphaGAN [30].

Methods	SAD	MSE	GRAD	CONN
Closed-Form Matting [8]	78.768	0.065	57.047	56.856
DCNN Matting [22]	85.842	0.070	57.622	65.196
Deep Matting [23]	33.075	0.017	23.316	34.204
IndexNet Matting [24]	28.984	0.013	19.127	28.872
Information-flow Matting [3]	84.766	0.067	52.789	63.827
KNN Matting [4]	95.122	0.082	66.188	74.940
Late Fusion [28]	88.109	0.097	59.382	91.743
AlphaGAN [30]	35.057	0.019	33.598	35.963
AlphaGan-BG_M	11.312	0.002	4.850	8.696
AlphaGan-BG_H	14.692	0.003	8.410	12.328

Table 1: The quantitative comparison of the AlphaGan-BG models against state of the art. The best average value/metric is emboldened.

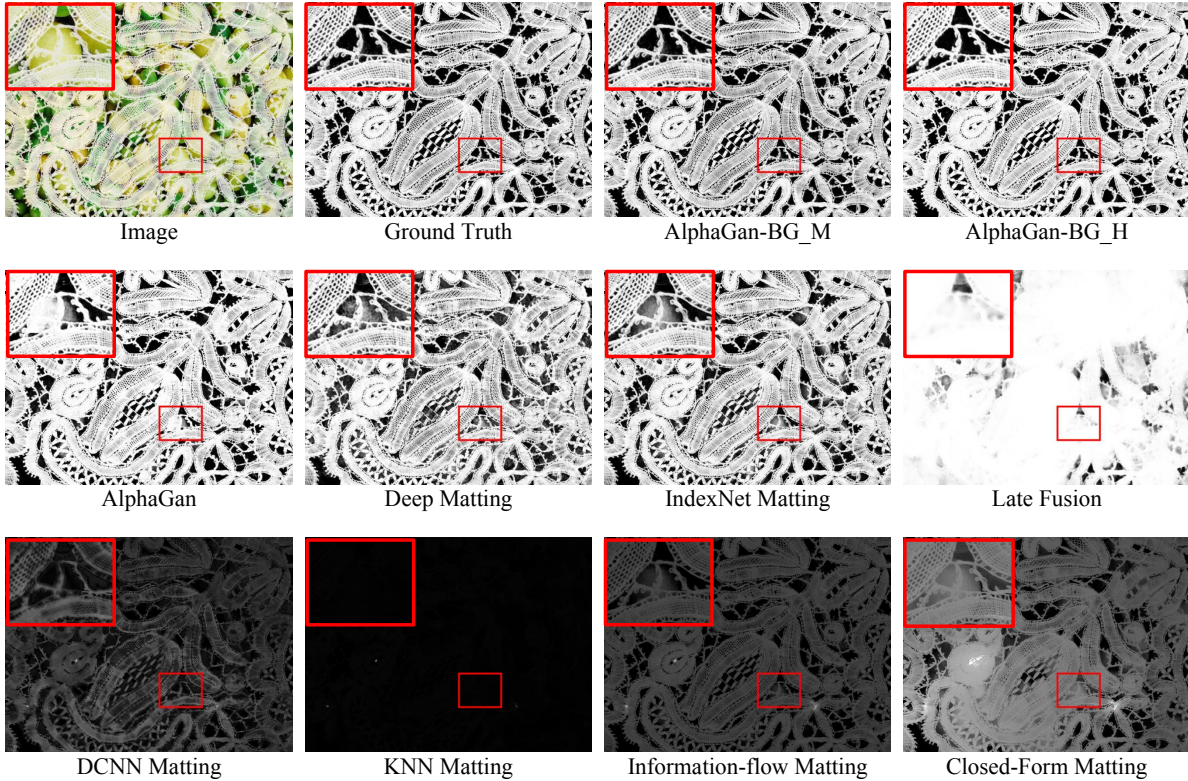


Figure 2: Comparison with State of the Art Methods - Example 1.

Table 1 presents the numerical evaluation of the AlphaGan-BG models against the state of the art methods and clearly notes that AlphaGan-BG outperforms the other methods based on the commonly used AlphaMatting benchmark metrics. This experiment also validates the idea of using background information for alpha estimation. As discussed in Section 4.2, based on the current state of the art in background reconstruction, it is very challenging to obtain a clear reconstructed background; However, this experiment demonstrates that even having a partial information about the background plane (with distortion) can significantly increase the accuracy of the alpha prediction.

Fig. 2 and Fig. 3 illustrate the qualitative comparison of the proposed models against the state of the art methods. A part of the predicted alpha mattes by the state of the art is marked in Fig. 2 to closely expose the difference in the performance of the methods.

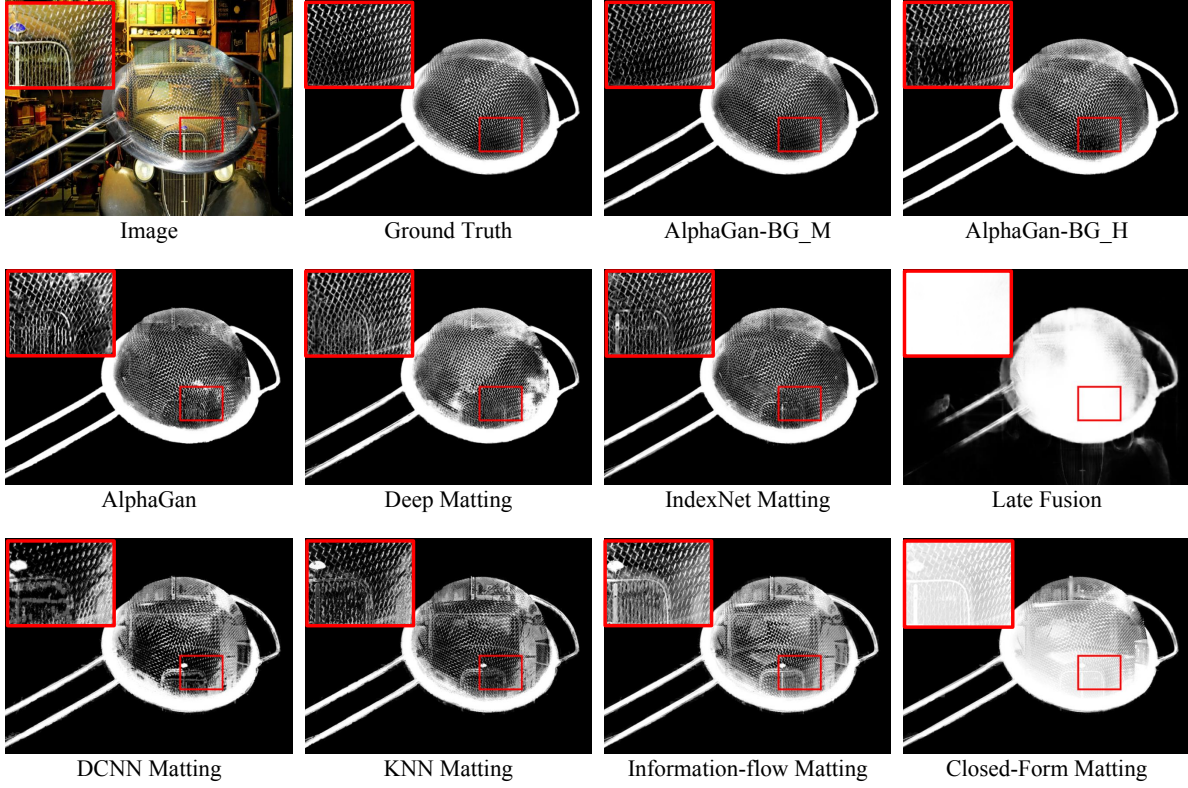


Figure 3: Comparison with State of the Art Methods - Example 2.

The performance of the AlphaGan-BG_M and AlphaGan-BG_H in Fig. 2 is a clear example and proof of an earlier statement that including the partial background information of the image during the matting pipeline, can significantly increase its accuracy and preserve fine details.

Fig. 3 is another example of the visual comparison against the state of the art where the superior performance of the AlphaGan-BG_M and AlphaGan-BG_H is clearly visible through the marked areas. For more and detailed visual results refer to Appendix 1.

4.6 Video Matting

To evaluate the performance of the AlphaGan-BG_M and AlphaGan-BG_H on video sequences, we used four state of the art background reconstruction and inpainting methods including Deep Video Inpainting (DVI) [41], Deep Flow Inpainting (DFGI) [42], FVC [50] and Gated Video Inpainting (GVI) [51] to separate the foreground and background layers. We also considered backgrounds with simulated artifacts as part of this evaluation. The background layers are further used as the input to the proposed matting framework. Three video sequences including *Alex*, *Castle* and *Dmitriy* from VideoMatting benchmark [52] are used for evaluation purposes. Tables 2-5 present the numerical evaluation of the AlphaGan-BG models on video sequences. The aforementioned reconstruction methods are applied to each sequence to extract the background layer as one of the input channels to AlphaGan-BG models. One important and obvious take from this experiment is the fact that a successful background aware matting method significantly relies on the quality of the reconstructed background. Although, the point of this experiment is not to compare the performance of the reconstruction methods, a few state of the art techniques such as FCV [50] generate background layers with less artifacts and similar to the simulated ones resulting in more accurate alpha estimation using AlphaGan-BG_M. On the other hand, AlphaGan-BG_H performs better in scenarios where the reconstructed background layers are heavily distorted such as DVI [41] and DFGI [42]. A detailed set of visual results for this section is provided in Appendix 2.

	W\Artifact			DVI [41]			DFGI [42]			GVI [51]			FVC [50]		
	A	C	D	A	C	D	A	C	D	A	C	D	A	C	D
AlphaGan-BG_M	1.004	10.145	1.66	9.95	95.712	11.856	1.787	32.808	2.28	16.814	89.4	15.046	1.165	11.385	1.781
AlphaGan-BG_H	1.28	28.062	1.758	1.658	53.513	2.115	1.292	37.207	1.775	2.409	56.7	2.91	1.3	28.352	1.77

Table 2: SAD Metric - Performance of the AlphaGan-BG models using different background reconstruction methods. A: Alex, C: Castle and D: Dimitriy. The best average value per model for each animation across all reconstruction method is emboldened.

	W\Artifact			DVI [41]			DFGI [42]			GVI [51]			FVC [50]		
	A	C	D	A	C	D	A	C	D	A	C	D	A	C	D
AlphaGan-BG_M	0.0001	0.001	0.0006	0.014	0.059	0.014	0.0008	0.014	0.001	0.027	0.053	0.019	0.0002	0.001	0.0007
AlphaGan-BG_H	0.0002	0.010	0.0008	0.0006	0.028	0.001	0.0003	0.017	0.0008	0.001	0.031	0.002	0.0003	0.011	0.0008

Table 3: MSE Metric - Performance of the AlphaGan-BG models using different background reconstruction methods. A: Alex, C: Castle and D: Dimitriy. The best average value per model for each animation across all reconstruction method is emboldened.

	W\Artifact			DVI [41]			DFGI [42]			GVI [51]			FVC [50]		
	A	C	D	A	C	D	A	C	D	A	C	D	A	C	D
AlphaGan-BG_M	0.365	5.779	2.51	12.52	123.945	21.397	1.376	33.184	3.931	17.57	110.25	25.134	0.582	7.826	2.835
AlphaGan-BG_H	0.744	67.829	3.059	1.075	95.806	4.061	0.766	75.408	3.099	2.111	97.737	6.213	0.762	68.364	3.098

Table 4: GRAD Metric - Performance of the AlphaGan-BG models using different background reconstruction methods. A: Alex, C: Castle and D: Dimitriy. The best average value per model for each animation across all reconstruction method is emboldened.

	W\Artifact			DVI [41]			DFGI [42]			GVI [51]			FVC [50]		
	A	C	D	A	C	D	A	C	D	A	C	D	A	C	D
AlphaGan-BG_M	0.457	7.77	1.562	9.78	100.104	11.932	1.21	33.173	2.131	17.066	93.838	15.254	0.624	9.208	1.68
AlphaGan-BG_H	0.801	27.864	1.707	1.252	55.5	2.085	0.818	37.95	1.725	2.162	58.965	2.948	0.825	28.191	1.719

Table 5: CONN Metric - Performance of the AlphaGan-BG models using different background reconstruction methods. A: Alex, C: Castle and D: Dimitriy. The best average value per model for each animation across all reconstruction method is emboldened.

5 Conclusion

In this paper we proposed an approach inspired by a state of the art GAN model to validate the idea of using background information as part of the alpha matting process. The proposed approach utilises an encoder-decoder structure as generator and PatchGAN as discriminator. The input to the network consists of 7 channels, including RGB image, RGB background information and the trimap. The preliminary results of the experiments and evaluations against the benchmarked methods indicate the validity of the core idea in this research. Using the full or partial background information, AlphaGan-BG demonstrated a superior performance against the studied methods. In the future work, we would like to train and analyse the performance of AlphaGan-BG on synthetic data. The background reconstruction process is another exciting aspect of this research that requires more investigation. The current performance of the models is achieved by simulating the reconstruction artifacts. However, we believe that AlphaGan-BG can obtain a higher accuracy if trained on a specific background reconstruction method with consistent noise and artifact pattern.

References

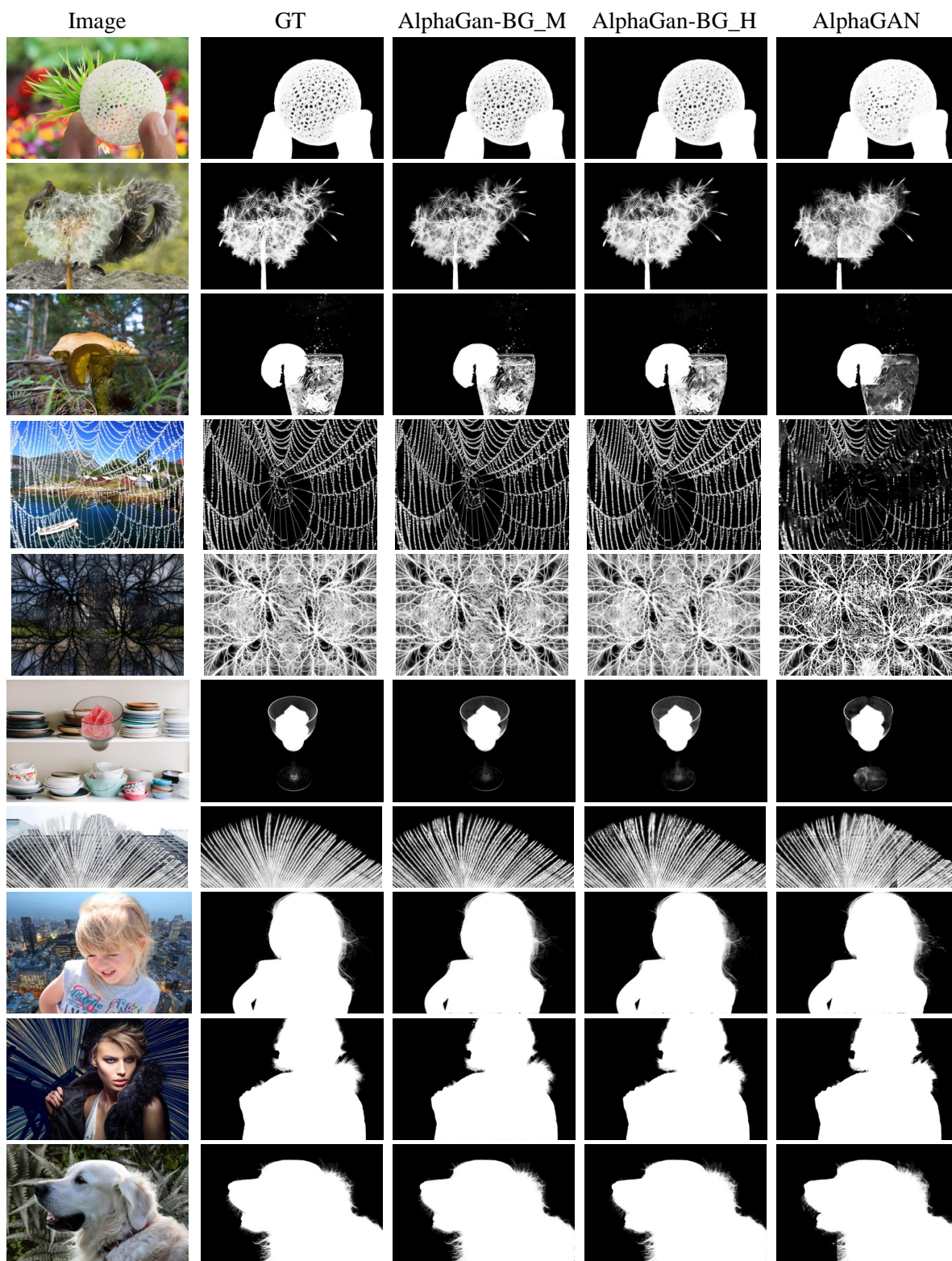
- [1] Yung-Yu Chuang et al. “A Bayesian approach to digital matting”. In: *2001 IEEE Conference on Computer Vision and Pattern Recognition (CVPR)*. Vol. 2. 2001, pp. 264–271. DOI: 10.1109/CVPR.2001.990970.
- [2] Jue Wang, Michael F Cohen, et al. “Image and video matting: a survey”. In: *Foundations and Trends® in Computer Graphics and Vision* 3.2 (2008), pp. 97–175.
- [3] Y. Aksoy, T. O. Aydin, and M. Pollefeys. “Designing Effective Inter-Pixel Information Flow for Natural Image Matting”. In: *2017 IEEE Conference on Computer Vision and Pattern Recognition (CVPR)*. 2017, pp. 228–236. DOI: 10.1109/CVPR.2017.32.
- [4] Q. Chen, D. Li, and C. Tang. “KNN Matting”. In: *IEEE Transactions on Pattern Analysis and Machine Intelligence* 35.9 (2013), pp. 2175–2188. ISSN: 1939-3539. DOI: 10.1109/TPAMI.2013.18.

- [5] X. Chen et al. “Image Matting with Local and Nonlocal Smooth Priors”. In: *2013 IEEE Conference on Computer Vision and Pattern Recognition*. 2013, pp. 1902–1907. DOI: 10.1109/CVPR.2013.248.
- [6] K. He, J. Sun, and X. Tang. “Fast matting using large kernel matting Laplacian matrices”. In: *2010 IEEE Computer Society Conference on Computer Vision and Pattern Recognition*. 2010, pp. 2165–2172. DOI: 10.1109/CVPR.2010.5539896.
- [7] P. Lee and Y. Wu. “Nonlocal matting”. In: *CVPR 2011*. 2011, pp. 2193–2200. DOI: 10.1109/CVPR.2011.5995665.
- [8] A. Levin, D. Lischinski, and Y. Weiss. “A Closed-Form Solution to Natural Image Matting”. In: *IEEE Transactions on Pattern Analysis and Machine Intelligence* 30.2 (2008), pp. 228–242. ISSN: 1939-3539. DOI: 10.1109/TPAMI.2007.1177.
- [9] A. Levin, A. Rav-Acha, and D. Lischinski. “Spectral Matting”. In: *IEEE Transactions on Pattern Analysis and Machine Intelligence* 30.10 (2008), pp. 1699–1712. ISSN: 1939-3539. DOI: 10.1109/TPAMI.2008.168.
- [10] Jian Sun et al. “Poisson Matting”. In: *ACM SIGGRAPH 2004 Papers*. SIGGRAPH ’04. Los Angeles, California: Association for Computing Machinery, 2004, 315–321. ISBN: 9781450378239. DOI: 10.1145/1186562.1015721. URL: <https://doi.org/10.1145/1186562.1015721>.
- [11] B. He et al. “Iterative transductive learning for alpha matting”. In: *2013 IEEE International Conference on Image Processing*. 2013, pp. 4282–4286. DOI: 10.1109/ICIP.2013.6738882.
- [12] K. He et al. “A global sampling method for alpha matting”. In: *CVPR 2011*. 2011, pp. 2049–2056. DOI: 10.1109/CVPR.2011.5995495.
- [13] J. Wang and M. F. Cohen. “An iterative optimization approach for unified image segmentation and matting”. In: *Tenth IEEE International Conference on Computer Vision (ICCV’05) Volume 1*. Vol. 2. 2005, 936–943 Vol. 2. DOI: 10.1109/ICCV.2005.37.
- [14] J. Wang and M. F. Cohen. “Optimized Color Sampling for Robust Matting”. In: *2007 IEEE Conference on Computer Vision and Pattern Recognition*. 2007, pp. 1–8. DOI: 10.1109/CVPR.2007.383006.
- [15] Eduardo Simoes Lopes Gastal and Manuel Menezes de Oliveira Neto. “Shared Sampling for Real-Time Alpha Matting”. In: *Comput. Graph. Forum* 29 (2010), pp. 575–584.
- [16] Xiaoxue Feng, Xiaohui Liang, and Zili Zhang. “A Cluster Sampling Method for Image Matting via Sparse Coding”. In: *Computer Vision – ECCV 2016*. Ed. by Bastian Leibe et al. Cham: Springer International Publishing, 2016, pp. 204–219. ISBN: 978-3-319-46475-6.
- [17] L. Karacan, A. Erdem, and E. Erdem. “Image Matting with KL-Divergence Based Sparse Sampling”. In: *2015 IEEE International Conference on Computer Vision (ICCV)*. 2015, pp. 424–432. DOI: 10.1109/ICCV.2015.56.
- [18] Xiaowu Chen et al. “Manifold Preserving Edit Propagation”. In: *ACM Trans. Graph.* 31.6 (Nov. 2012). ISSN: 0730-0301. DOI: 10.1145/2366145.2366151. URL: <https://doi.org/10.1145/2366145.2366151>.
- [19] Leo Grady et al. “Random walks for interactive alpha-matting”. In: *Proceedings of VIIP*. Vol. 2005. 2005, pp. 423–429.
- [20] Yuanjie Zheng et al. “FuzzyMatte: A computationally efficient scheme for interactive matting”. In: *2008 IEEE Conference on Computer Vision and Pattern Recognition*. 2008, pp. 1–8. DOI: 10.1109/CVPR.2008.4587455.
- [21] X. Bai and G. Sapiro. “A Geodesic Framework for Fast Interactive Image and Video Segmentation and Matting”. In: *2007 IEEE 11th International Conference on Computer Vision*. 2007, pp. 1–8. DOI: 10.1109/ICCV.2007.4408931.
- [22] Donghyeon Cho, Yu-Wing Tai, and Inso Kweon. “Natural Image Matting Using Deep Convolutional Neural Networks”. In: *Computer Vision – ECCV 2016*. Ed. by Bastian Leibe et al. Cham: Springer International Publishing, 2016, pp. 626–643. ISBN: 978-3-319-46475-6.
- [23] N. Xu et al. “Deep Image Matting”. In: *2017 IEEE Conference on Computer Vision and Pattern Recognition (CVPR)*. 2017, pp. 311–320. DOI: 10.1109/CVPR.2017.41.
- [24] Hao Lu et al. “Indices Matter: Learning to Index for Deep Image Matting”. In: *The IEEE International Conference on Computer Vision (ICCV)*. 2019.
- [25] H. Tang et al. “Very Deep Residual Network for Image Matting”. In: *2019 IEEE International Conference on Image Processing (ICIP)*. 2019, pp. 4255–4259. DOI: 10.1109/ICIP.2019.8803682.
- [26] Jingwei Tang et al. “Learning-Based Sampling for Natural Image Matting”. In: *The IEEE Conference on Computer Vision and Pattern Recognition (CVPR)*. 2019.
- [27] Shaofan Cai et al. “Disentangled Image Matting”. In: *The IEEE International Conference on Computer Vision (ICCV)*. 2019.
- [28] Yunke Zhang et al. “A Late Fusion CNN for Digital Matting”. In: *The IEEE Conference on Computer Vision and Pattern Recognition (CVPR)*. 2019.

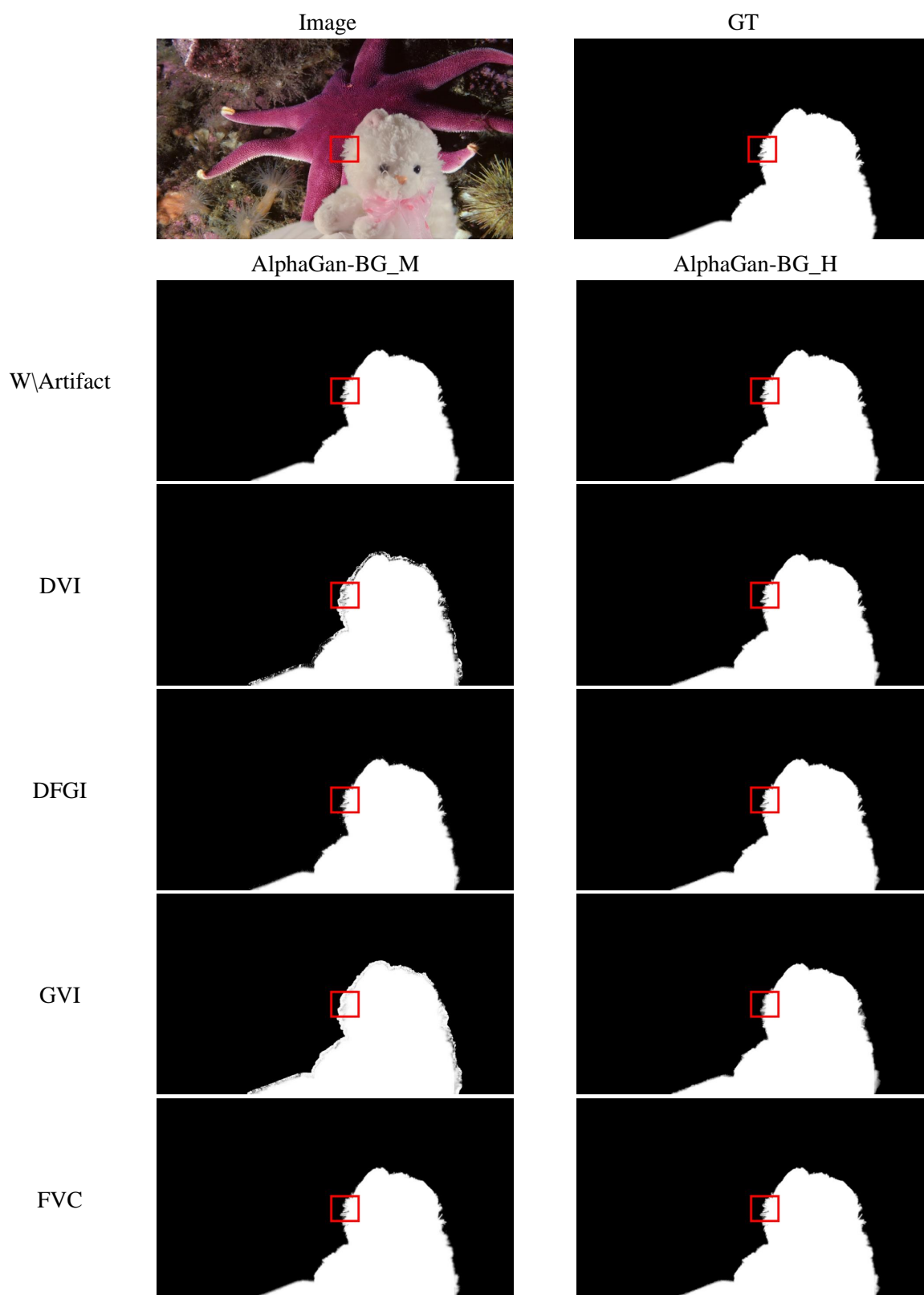
- [29] Yaoyi Li et al. “Inductive Guided Filter: Real-time Deep Image Matting with Weakly Annotated Masks on Mobile Devices”. In: *CoRR* abs/1905.06747 (2019). arXiv: 1905.06747. URL: <http://arxiv.org/abs/1905.06747>.
- [30] Sebastian Lutz, Konstantinos Amplianitis, and Aljosa Smolic. “AlphaGAN: Generative adversarial networks for natural image matting”. In: *2018 British Machine Vision Conference, Northumbria University, Newcastle, UK*. Sep 2018, p. 259. URL: <http://bmvc2018.org/contents/papers/0915.pdf>.
- [31] K. He et al. “Deep Residual Learning for Image Recognition”. In: *2016 IEEE Conference on Computer Vision and Pattern Recognition (CVPR)*. 2016, pp. 770–778. DOI: 10.1109/CVPR.2016.90.
- [32] Olga Russakovsky et al. “ImageNet Large Scale Visual Recognition Challenge”. In: *Int. J. Comput. Vision* 115.3 (Dec. 2015), 211–252. ISSN: 0920-5691. DOI: 10.1007/s11263-015-0816-y. URL: <https://doi.org/10.1007/s11263-015-0816-y>.
- [33] Liang-Chieh Chen et al. “Rethinking Atrous Convolution for Semantic Image Segmentation”. In: *CoRR* abs/1706.05587 (2017). arXiv: 1706.05587. URL: <http://arxiv.org/abs/1706.05587>.
- [34] L. Chen et al. “DeepLab: Semantic Image Segmentation with Deep Convolutional Nets, Atrous Convolution, and Fully Connected CRFs”. In: *IEEE Transactions on Pattern Analysis and Machine Intelligence* 40.4 (2018), pp. 834–848. ISSN: 1939-3539. DOI: 10.1109/TPAMI.2017.2699184.
- [35] Vinod Nair and Geoffrey E. Hinton. “Rectified Linear Units Improve Restricted Boltzmann Machines”. In: *Proceedings of the 27th International Conference on International Conference on Machine Learning*. ICML 10. Haifa, Israel: Omnipress, 2010, 807–814. ISBN: 9781605589077.
- [36] Sergey Ioffe and Christian Szegedy. “Batch Normalization: Accelerating Deep Network Training by Reducing Internal Covariate Shift”. In: *Proceedings of the 32nd International Conference on International Conference on Machine Learning - Volume 37*. ICML’15. Lille, France: JMLR.org, 2015, 448–456.
- [37] P. Isola et al. “Image-to-Image Translation with Conditional Adversarial Networks”. In: *2017 IEEE Conference on Computer Vision and Pattern Recognition (CVPR)*. 2017, pp. 5967–5976. DOI: 10.1109/CVPR.2017.632.
- [38] Ian Goodfellow et al. “Generative Adversarial Nets”. In: *Advances in Neural Information Processing Systems* 27. Ed. by Z. Ghahramani et al. Curran Associates, Inc., 2014, pp. 2672–2680. URL: <http://papers.nips.cc/paper/5423-generative-adversarial-nets.pdf>.
- [39] Mark Everingham et al. “The pascal visual object classes (voc) challenge”. In: *International journal of computer vision* 88.2 (2010), pp. 303–338.
- [40] Tsung-Yi Lin et al. “Microsoft coco: Common objects in context”. In: *European conference on computer vision*. Springer, 2014, pp. 740–755.
- [41] D. Kim et al. “Deep Video Inpainting”. In: *2019 IEEE/CVF Conference on Computer Vision and Pattern Recognition (CVPR)*. 2019, pp. 5785–5794. DOI: 10.1109/CVPR.2019.00594.
- [42] R. Xu et al. “Deep Flow-Guided Video Inpainting”. In: *2019 IEEE/CVF Conference on Computer Vision and Pattern Recognition (CVPR)*. 2019, pp. 3718–3727. DOI: 10.1109/CVPR.2019.00384.
- [43] Jia-Bin Huang et al. “Temporally Coherent Completion of Dynamic Video”. In: *ACM Trans. Graph.* 35.6 (Nov. 2016). ISSN: 0730-0301. DOI: 10.1145/2980179.2982398. URL: <https://doi.org/10.1145/2980179.2982398>.
- [44] Benjamin Laugraud, Sébastien Piérard, and Marc Van Droogenbroeck. “LaBGen: A method based on motion detection for generating the background of a scene”. In: *Pattern Recognition Letters* 96 (2017). Scene Background Modeling and Initialization, pp. 12–21. ISSN: 0167-8655. DOI: <https://doi.org/10.1016/j.patrec.2016.11.022>. URL: <http://www.sciencedirect.com/science/article/pii/S0167865516303439>.
- [45] Benjamin Laugraud et al. “Simple Median-Based Method for Stationary Background Generation Using Background Subtraction Algorithms”. In: *New Trends in Image Analysis and Processing – ICIAP 2015 Workshops*. Ed. by Vittorio Murino et al. Cham: Springer International Publishing, 2015, pp. 477–484. ISBN: 978-3-319-23222-5.
- [46] J. Herling and W. Broll. “High-Quality Real-Time Video Inpainting with PixMix”. In: *IEEE Transactions on Visualization and Computer Graphics* 20.6 (2014), pp. 866–879. ISSN: 2160-9306. DOI: 10.1109/TVCG.2014.2298016.
- [47] Diederik P Kingma and Jimmy Ba. “Adam: A method for stochastic optimization”. In: *arXiv preprint arXiv:1412.6980* (2014).
- [48] C. Rhemann et al. “A perceptually motivated online benchmark for image matting”. In: *2009 IEEE Conference on Computer Vision and Pattern Recognition*. 2009, pp. 1826–1833. DOI: 10.1109/CVPR.2009.5206503.
- [49] *Alpha Matting Evaluation Website*. URL: <http://www.alphamatting.com/> (visited on 01/13/2020).
- [50] M. Afifi et al. “Fast Video Completion using patch-based synthesis and image registration”. In: *2014 International Symposium on Intelligent Signal Processing and Communication Systems (ISPACS)*. 2014, pp. 200–204. DOI: 10.1109/ISPACS.2014.7024452.

- [51] Ya-Liang Chang et al. “Free-form Video Inpainting with 3D Gated Convolution and Temporal PatchGAN”. In: *In Proceedings of the International Conference on Computer Vision (ICCV)* (2019).
- [52] Mikhail Erofeev et al. “Perceptually Motivated Benchmark for Video Matting”. In: *Proceedings of the British Machine Vision Conference (BMVC)*. BMVA Press, 2015, pp. 99.1–99.12. ISBN: 1-901725-53-7. DOI: 10.5244/C.29.99. URL: <https://dx.doi.org/10.5244/C.29.99>.

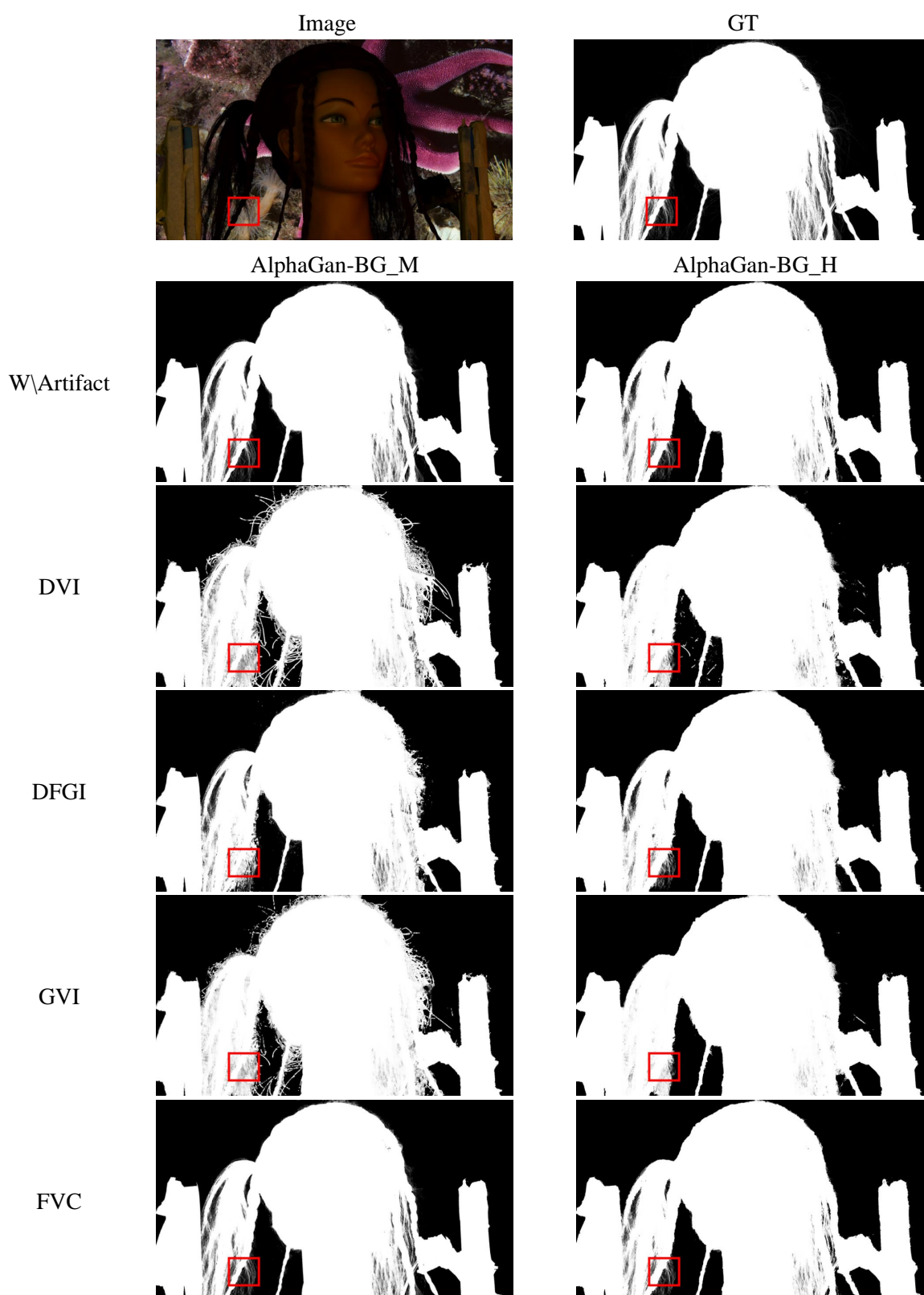
Appendix 1: Visual Results on Adobe Matting dataset



Appendix 2: Visual Results on Video Matting dataset - A Frame from Alex Video Sequence



Appendix 2: Visual Results on Video Matting dataset - A Frame from Castle Video Sequence



Appendix 2: Visual Results on Video Matting dataset - A Frame from Dmitriy Video Sequence

